Multicenter approach to the exchange-correlation interactions in *ab initio* tight-binding methods

Pavel Jelínek,[1,2] Hao Wang,[3] James P. Lewis,[3] Otto F. Sankey,[4] and José Ortega[1]
[1]*Departamento de Física Teórica de la Materia Condensada, Universidad Autónoma de Madrid, Madrid E-28049 Spain*
[2]*Institute of Physics, Academy of Sciences of the Czech Republic, Cukrovarnická 10, 1862 53, Prague, Czech Republic*
[3]*Department of Physics and Astronomy, Brigham Young University, Provo, Utah 84602-4658, USA*
[4]*Department of Physics and Astronomy, Arizona State University, Tempe, Arizona 85287-1504, USA*
(Received 21 September 2004; revised manuscript received 21 December 2004; published 6 June 2005)

An approximate method to calculate exchange-correlation contributions in the framework of first-principles tight-binding molecular dynamics methods has been developed. In the proposed scheme on-site (off-site) exchange-correlation matrix elements are expressed as a one-center (two-center) term plus a correction due to other neighboring atoms. The one-center (two-center) term is evaluated directly, while the correction is calculated using a generalization of the [Sankey-Niklewski Phys. Rev. B **40**, 3979 (1989)] approach valid for arbitrary atomiclike basis sets. The proposed scheme for exchange-correlation terms, called the multi-center weighted exchange-correlation density approximation (McWEDA), permits the accurate and computationally efficient calculation of corresponding tight-binding matrices and atomic forces for complex systems. We calculate bulk properties of selected transition (W,Pd), noble (Au), and simple (Al) metals, a semiconductor (Si), and the transition metal oxide TiO_2 with the method to demonstrate its flexibility and accuracy.

DOI: 10.1103/PhysRevB.71.235101 PACS number(s): 71.15.Ap, 31.10.+z

I. INTRODUCTION

The application of first-principles simulation techniques is becoming a research tool of increasing importance in materials science, condensed matter physics and chemistry, and molecular physics and chemistry. Most of these techniques are based on density functional theory[2] (DFT) which creates an important simplification of the many-body quantum-mechanical problem. Typically, DFT calculations are performed within the Kohn-Sham approach[3] using the local density approximation (LDA)[3] or a generalized gradient approximation (GGA).[4] These total-energy quantum-mechanical methods can be used to calculate forces on atoms, and thus perform first-principles molecular dynamics (MD) simulations. Such simulations have been very successful in the description of a variety of properties of different materials. However, in spite of the important simplifications introduced by DFT and related approximations (e.g., LDA,GGA), complex systems still require huge computational resources. This problem has severely limited the range of applications of these simulation techniques to situations with small numbers of atoms ($\sim 100-200$) in the unit cell, and short MD simulation times.

Due to the computational limitations, first-principles simulation techniques have been mainly directed to the study of the energetics and electronic structure of diverse materials, surfaces, and molecules. Typically, a good guess for the atomic structure is obtained before the calculation, and the first-principles method is then used to refine the geometry, obtain the electronic structure, and compare the total energy of a few competing structures. These methods, however, have been very rarely applied to elucidate complex atomic structures that require the *exploration* of an extensive phase space of possibilities when no *a priori* answer, or approximate good guess, is already available. More importantly, the application of first-principles methods to investigate complex kinetic processes in materials (e.g., the atomic motion of atoms on a surface, kinetic pathways, molecular reactions, etc.) is still very limited, due to the computational resources required for these calculations.

It is clear that the usefulness of first-principles simulation techniques can be greatly extended if appropriate approximations are made, with the purpose of increasing the computational efficiency, with as little loss of accuracy as possible.[1,5–9] This idea has prompted the development of first-principles tight-binding molecular dynamics (TBMD) methods,[1,5,10] whose main characteristics are (1) a *real-space* technique (i.e., no need for supercells or grids), (2) *optimized atomiclike orbitals*[1,5,11,12] as basis set, and (3) efficient, two-dimensional, tabulation-interpolation schemes[1,5] to obtain the effective TB Hamiltonian matrix elements as well as their derivatives to obtain the forces.

The main advantage of such techniques is computational efficiency which makes them ideal first-principles exploratory tools. The use of first-principles TBMD methods as a exploratory tool can be complemented with more accurate calculations, if necessary; once stimulating results and/or new ideas are obtained, final results can be refined by performing more accurate and time-consuming calculations (plane-wave DFT, e.g., Ref. 13, or even many-body, e.g., Ref. 14, calculations).

In this paper we report on further developments for the efficient calculation of exchange-correlation contributions in first-principles TBMD methods, and their implementation in the FIREBALL code.[1,15,16] The basic theoretical elements of this technique are briefly reviewed in Sec. II, including a more detailed analysis of the two different approximations previously proposed[1,5] for the practical calculation of exchange-correlation matrix elements in these methods using standard DFT (e.g., LDA). The LDA (or GGA) exchange-correlation energy is highly nonlinear in the electron density and this presents special difficulties in the creation of accurate and efficient approximate methods. In Sec. III we

present our methodology to calculate these contributions: this approach overcomes the main deficiencies of the previous approximations (discussed in Sec. II), mixing accuracy and computational efficiency. Finally, in Sec. IV we present results for several materials (Al, Si, Au, W, Pd, TiO_2) that illustrate the good performance of this approach.

II. *AB INITIO* TIGHT BINDING: FIREBALL

FIREBALL[1,15,16] is a first-principles TBMD simulation technique based on a self-consistent version of the Harris-Foulkes[17,18] functional. The energy functional is written as

$$E_{\text{tot}}[\rho(\vec{r})] = \sum_n \varepsilon_n - E_{ee}[\rho(\vec{r})] + E_{\text{xc}}[\rho(\vec{r})] - \int \rho(\vec{r}) V_{\text{xc}}[\rho(\vec{r})] d^3r + E_{\text{ion-ion}}, \quad (1)$$

where $\rho(\vec{r})$ is the *input density*, which will be allowed to vary, and will be determined self-consistently. The first term is a sum over occupied eigenstates ε_n of the effective one-electron Hamiltonian,

$$\left(-\frac{1}{2}\nabla^2 + V[\rho]\right)\psi_n = \varepsilon_n \psi_n; \quad (2)$$

the potential V is the sum of the ionic potential $v_{\text{ion}}(\vec{r})$ (typically represented by a pseudopotential), a Hartree potential, and an exchange-correlation potential V_{xc},

$$V[\rho] = v_{\text{ion}}(\vec{r}) + \int \frac{\rho(r')d^3r'}{|\vec{r}-\vec{r}'|} + V_{\text{xc}}[\rho(\vec{r})]. \quad (3)$$

In Eq. (1) E_{ee} is an average electron-electron energy,

$$E_{ee}[\rho] = \frac{1}{2}\int\int \frac{\rho(\vec{r})\rho(\vec{r}')}{|\vec{r}-\vec{r}'|} d\vec{r}\, d\vec{r}', \quad (4)$$

$E_{\text{ion-ion}}$ is the ion-ion interaction energy,

$$E_{\text{ion-ion}} = \frac{1}{2}\sum_{i,j} \frac{Z_i Z_j}{|\vec{R}_i - \vec{R}_j|} \quad (5)$$

(Z_i is the nuclear or pseudopotential charge of atom i at position $\vec{R}_i$), and $E_{\text{xc}}[\rho]$ is the exchange-correlation energy. First-principles MD simulations can be performed once the forces

$$\vec{F}_i = -\frac{\partial E_{\text{tot}}}{\partial \vec{R}_i} \quad (6)$$

on each atom i are evaluated.

The efficiency of calculations based on the Harris-Foulkes functional is associated with the possibility to choose $\rho(\vec{r})$ in the above equations as a sum of atomiclike densities $\rho_i(\vec{r})$,

$$\rho(\vec{r}) = \sum_i \rho_i(\vec{r}). \quad (7)$$

In the FIREBALL method, confined atomiclike orbitals are used as a basis set for the determination of the occupied eigenvalues and eigenvectors of the one-electron Hamiltonian, Eq. (2). The fireball orbitals, introduced by Sankey and Niklewski (SN),[1] are obtained by solving the atomic problem with the boundary condition that the atomic orbitals vanish outside and at a predetermined radius r_c where $\psi(\vec{r})|_{r=r_c} = 0$. An important advantage of the fireball basis set is that the Hamiltonian [Eq. (2)] and the overlap matrix elements are quite sparse for large systems. The electron density $\rho(\vec{r})$ is written in terms of the fireball orbitals $\phi_{ilm}(\vec{r}) \equiv \phi_\mu(\vec{r})$ (i is the atomic site, l represents the atomic subshell, e.g., $3s, 4s, 3p, 3d$, etc., and m is the magnetic quantum number)

$$\rho(\vec{r}) = \sum_\mu q_\mu |\phi_\mu(\vec{r})|^2. \quad (8)$$

In this way four-center integrals are not required for the calculation of the Hartree terms, and all the two- and three-center interactions are tabulated beforehand and placed in interpolation data tables which are no larger than two dimensional.[1] Hamiltonian matrix elements are evaluated by looking up the necessary information from the data tables.

In practice, the atomic densities ρ_i

$$\rho_i(\vec{r}) = \sum_{lm} q_{ilm} |\phi_{ilm}(\vec{r})|^2 \quad (9)$$

are approximated to be spherically symmetric around each atomic site i (i.e., $q_{ilm} = q_{ilm'}$). Self-consistency is achieved by imposing that the output orbital charges q_μ^{out} [obtained from the occupied eigenvectors ψ_n of Eq. (2)] and input orbital charges q_μ coincide (see Refs. 15 and 19 for further details).

The remaining difficulty is the efficient calculation of exchange-correlation interactions within a first-principles TB scheme. One possibility is to use nonstandard DFT and introduce the exchange-correlation energy and potential as a function of the orbital occupancies.[9,20,21] In this paper, however, we opt for the more traditional approach in which exchange-correlation contributions are calculated as a functional of the electron density $\rho(\vec{r})$. Within this line, two different methods have been previously proposed for the practical calculation of exchange-correlation terms, using data tables similar to those for the Hartree contributions. These two methods are (A) the Sankey-Niklewski approximation, and (B) the Horsfield approximation.

A. Sankey-Niklewski approximation

The basic idea introduced by SN is to write down the nonlinear-in-$\rho(\vec{r})$ exchange-correlation matrix elements in terms of matrix elements of $\rho(\vec{r})$.[1] These latter matrix elements are easily tabulated in data tables no larger than two dimensional, similar to those required for the Hartree terms.

Consider the matrix elements $\langle \phi_\mu | V_{\text{xc}}[\rho] | \phi_\nu \rangle$ of the exchange-correlation potential. For each matrix element $\langle \phi_\mu | V_{\text{xc}}[\rho] | \phi_\nu \rangle$, expand $V_{\text{xc}}[\rho]$ in a Taylor series

$$V_{\text{xc}}[\rho] \simeq V_{\text{xc}}[\overline{\rho}_{\mu\nu}] + V'_{\text{xc}}[\overline{\rho}_{\mu\nu}](\rho - \overline{\rho}_{\mu\nu}) + \cdots \quad (10)$$

around an appropriate "average density" $\overline{\rho}_{\mu\nu}$:

$$\overline{\rho}_{\mu\nu} = \frac{\langle\phi_\mu|\rho|\phi_\nu\rangle}{\langle\phi_\mu|\phi_\nu\rangle}. \tag{11}$$

With this choice of $\overline{\rho}_{\mu\nu}$ the second term in the expansion for $\langle\phi_\mu|V_{xc}[\rho]|\phi_\nu\rangle$ is zero, and the next term is minimized.[1] This yields

$$\langle\phi_\mu|V_{xc}[\rho]|\phi_\nu\rangle \equiv \langle\mu|V_{xc}[\rho]|\nu\rangle \simeq V_{xc}[\overline{\rho}_{\mu\nu}]\langle\mu|\nu\rangle + C_{\mu\nu}, \tag{12}$$

where $C_{\mu\nu}$ are some corrections associated with the linear term in Eq. (10) [see Eqs. (40), (41), (42), and (45) in Ref. 1].

The SN definition of $\overline{\rho}_{\mu\nu}$ is based on the idea of "importance sampling;" the density is weighted more heavily in regions of higher overlap.[1] This is achieved by using the orbitals ϕ_μ as *weighting functions* in Eq. (11).

There are some deficiencies attributed to the SN method that we now discuss. First, note that $\overline{\rho}_{\mu\nu}$ in Eq. (11) is not defined in the zero-overlap case ($\langle\phi_\mu|\phi_\nu\rangle \equiv \langle\mu|\nu\rangle = 0$) when regions of positive and negative overlap "cancel out" (e.g., $\langle s|p_\pi\rangle$, or $\langle s|s'\rangle$ with two orthogonal s orbitals on the same atom). Second, in some extreme cases the sign of $\langle\mu|\rho|\nu\rangle$ may be different from the sign of $\langle\mu|\nu\rangle$. Third, in the SN method the average density approximation overestimates the exchange-correlation energy on-site terms $\langle\mu|\epsilon_{xc}|\mu\rangle$ [see Fig. 1(a)]. Finally, the SN method was originally proposed for minimal sp^3 basis sets (i.e., $\overline{\rho}_{\mu\nu}$ and $C_{\mu\nu}$ were only derived for sp^3 basis sets). An important ingredient in our approach to calculate exchange-correlation terms for TBMD (see Sec. III) will be to generalize the SN approximation for arbitrary atomiclike basis sets.

B. Horsfield approximation

An alternative approach to deal with exchange-correlation terms within a first-principles TBMD method was proposed by Horsfield,[5] who introduced a many-center expansion based on Eq. (7). In this approach we can distinguish two cases (i_μ is the atomic site corresponding to orbital μ and i_ν corresponds to orbital ν):

(a) $i_\mu = i_\nu \equiv i$ (on-site),

$$\langle\mu|V_{xc}[\rho]|\nu\rangle \simeq \langle\mu|V_{xc}[\rho_i]|\nu\rangle + \sum_{j\neq i}\langle\mu|(V_{xc}[\rho_i+\rho_j] - V_{xc}[\rho_i])|\nu\rangle; \tag{13}$$

(b) $(i_\mu \equiv i) \neq (i_\nu \equiv j)$ (off-site),

$$\langle\mu|V_{xc}[\rho]|\nu\rangle = \langle\mu|V_{xc}[\rho_i+\rho_j]|\nu\rangle + \sum_{k\neq i,j}\langle\mu|(V_{xc}[\rho_i+\rho_j+\rho_k] - V_{xc}[\rho_i+\rho_j])|\nu\rangle. \tag{14}$$

Although practical experience has shown that this is an accurate approach in many cases, the on-site terms [case (a)] are not always well approximated by Eq. (13) and it is necessary to perform the additional numerical integrals[5,6]

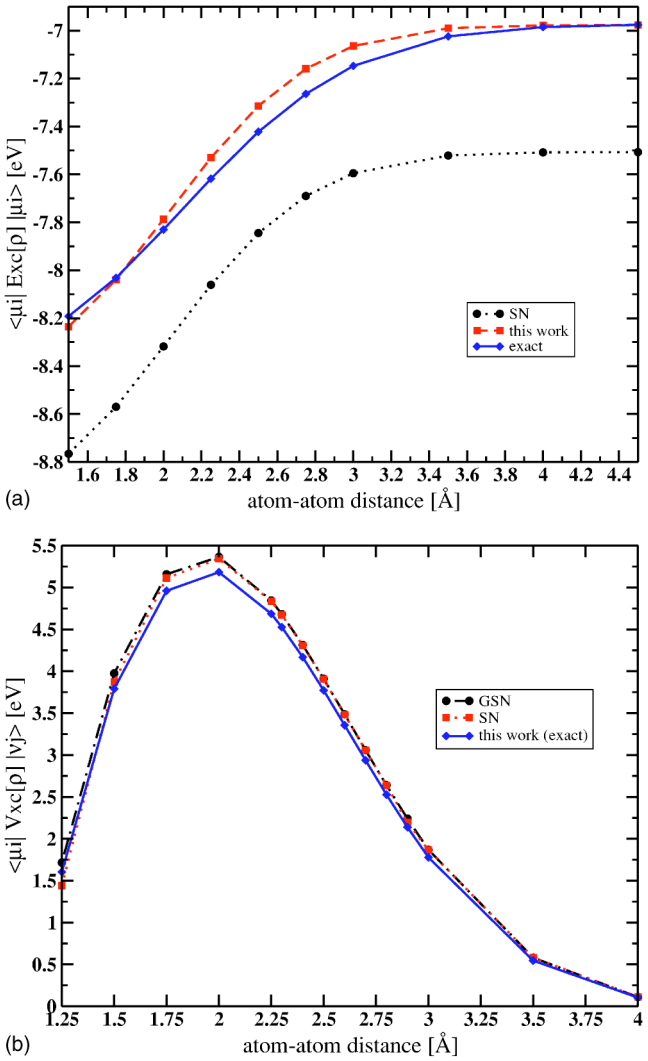

FIG. 1. (Color online) Exchange-correlation matrix elements for the Si dimer (along the z axis) as a function of distance. "This work" refers to the McWEDA approach. (a) On-site $\langle p_z|\epsilon_{xc}|p_z\rangle$ matrix element. (b) Off-site $\langle p_z|V_{xc}|p_z\rangle$ matrix element. Basis set: sp^3 fireball orbitals with cutoff radii $R_c(s) = 4.8$ a.u., $R_c(p) = 5.4$ a.u.

$$\langle\mu|\left(V_{xc}[\rho] - V_{xc}[\rho_i] - \sum_{j\neq i}(V_{xc}[\rho_i+\rho_j] - V_{xc}[\rho_i])\right)|\nu\rangle, \tag{15}$$

which cannot be obtained from data tables. Another shortcoming of this approach is the fact that most of the computational time required to create the data tables within this approximation is spent in the calculation of the exchange-correlation terms, reducing the computational efficiency.[22]

III. MULTICENTER EXCHANGE-CORRELATION SCHEME FOR *AB INITIO* TIGHT BINDING

In this section we present our approach for calculating exchange-correlation contributions in first-principles TBMD methods. Our goal is to introduce a practical scheme that overcomes the main deficiencies of the previous approaches, mixing accuracy and computational efficiency. For this pur-

pose, we use the best features of the SN and the Horsfield approximations. As in the Horsfield scheme, we distinguish two cases: (a) on-site ($i_\mu = i_\nu$) and (b) off-site matrix elements. For clarity, we discuss first case (a), and postpone to the end of the section the corresponding results for case (b).

(a) $i_\mu = i_\nu \equiv i$. As a first step in our approximation, we simply add and subtract a contribution associated with the atomic density ρ_i at site i, and write, *formally*, the matrix element as a one-center contribution plus a *correction*, in similarity with the Horsfield approach:

$$\langle\mu|V_{\rm xc}[\rho]|\nu\rangle = \langle\mu|V_{\rm xc}[\rho_i]|\nu\rangle + (\langle\mu|V_{\rm xc}[\rho]|\nu\rangle - \langle\mu|V_{\rm xc}[\rho_i]|\nu\rangle). \tag{16}$$

The one-center term (first term on the right) is much larger than the *correction* (inside parentheses), and is calculated exactly. The correction is calculated using a generalized version of the SN approach that we now discuss.

In order to generalize the SN approach beyond sp^3 basis sets, and correct the problems outlined in Sec. II, we define average densities $\overline{\rho}_{\mu\nu}$ using new *weighting functions* w_μ, associated with orbitals ϕ_μ, that are positive defined while keeping the importance-sampling property that the orbitals ϕ_μ play in Eq. (11). These functions are defined as follows. First, we consider the atomiclike orbitals

$$\phi_{ilm} = R_{il}(r)Y_{lm}(\Omega) \tag{17}$$

where $R_{il}(r)$ is the radial part of ϕ_{ilm} and $Y_{lm}(\Omega)$ the spherical harmonic associated with the angular part. Next, we define the new weighting functions

$$w_{il} = |R_{il}(r)|Y_{00}(\Omega) \tag{18}$$

[$|R_{il}(r)|$ is the absolute value of $R_{il}(r)$]. With these functions we now define average densities for each matrix element (μ, ν) as

$$\overline{\rho}_{\mu\nu} = \frac{\langle w_\mu|\rho|w_\nu\rangle}{\langle w_\mu|w_\nu\rangle}. \tag{19}$$

This definition for the average multisite densities $\overline{\rho}_{\mu\nu}$ (using weighting functions w instead of the atomic orbitals ϕ) (Ref. 23) solves all problems related to zero overlap ($\langle\phi_\mu|\phi_\nu\rangle = 0$) mentioned in Sec. II, since now $\langle w_\mu|w_\nu\rangle \neq 0$. Also, the use of these weighting functions represents, in general, an improvement in the "importance-sampling" calculation of $\overline{\rho}_{\mu\nu}$ for the nonzero-overlap cases. Regions of positive overlap are no longer "artificially" canceled by regions of negative overlap; both positive and negative overlap regions add up now in this definition of $\overline{\rho}_{\mu\nu}$. Moreover, with this definition for the weighting functions both $\langle w_\mu|\rho|w_\nu\rangle$ and $\langle w_\mu|w_\nu\rangle$ are positive thus assuring that $\overline{\rho}_{\mu\nu}$ is always well defined.

Using this definition of $\overline{\rho}_{\mu\nu}$ [Eq. (19)], we now define a *generalized* SN (GSN) approximation for the exchange-correlation matrix elements

$$\langle\mu|V_{\rm xc}[\rho]|\nu\rangle \simeq V_{\rm xc}[\overline{\rho}_{\mu\nu}]\langle\mu|\nu\rangle + V'_{\rm xc}[\overline{\rho}_{\mu\nu}](\langle\mu|\rho|\nu\rangle - \overline{\rho}_{\mu\nu}\langle\mu|\nu\rangle). \tag{20}$$

This approximation allows us to calculate the correction in Eq. (16), $(\langle\mu|V_{\rm xc}[\rho]|\nu\rangle - \langle\mu|V_{\rm xc}[\rho_i]|\nu\rangle)$, in a practical way.

Thus, we finally obtain the multicenter weighted exchange-correlation density approximation (McWEDA) for the on-site matrix elements,

$$\begin{aligned}\langle\mu|V_{\rm xc}[\rho]|\nu\rangle \simeq{}& \langle\mu|V_{\rm xc}[\rho_i]|\nu\rangle + V_{\rm xc}[\overline{\rho}_{\mu\nu}]\langle\mu|\nu\rangle + V'_{\rm xc}[\overline{\rho}_{\mu\nu}]\\ &\times(\langle\mu|\rho|\nu\rangle - \overline{\rho}_{\mu\nu}\langle\mu|\nu\rangle) - V_{\rm xc}[\overline{\rho_i}]\langle\mu|\nu\rangle\\ &- V'_{\rm xc}[\overline{\rho_i}](\langle\mu|\rho_i|\nu\rangle - \overline{\rho_i}\langle\mu|\nu\rangle)\end{aligned} \tag{21}$$

with

$$\overline{\rho_i} = \frac{\langle w_\mu|\rho_i|w_\nu\rangle}{\langle w_\mu|w_\nu\rangle} \tag{22}$$

(indices μ, ν have been omitted in $\overline{\rho_i}$, for clarity).

(b) $(i_\mu = i) \neq (i_\nu = j)$. Proceeding in a similar manner as for the on-site matrix elements, we first write the matrix element as a two-center main contribution, that we calculate exactly, and a correction that is evaluated using the GSN approximation. We obtain for the McWEDA evaluation of the off-site matrix elements

$$\begin{aligned}\langle\mu|V_{\rm xc}[\rho]|\nu\rangle = {}& \langle\mu|V_{\rm xc}[\rho_i + \rho_j]|\nu\rangle + (\langle\mu|V_{\rm xc}[\rho]|\nu\rangle\\ &- \langle\mu|V_{\rm xc}[\rho_i + \rho_j]|\nu\rangle)\end{aligned} \tag{23}$$

$$\begin{aligned}\simeq{}& \langle\mu|V_{\rm xc}[\rho_i + \rho_j]|\nu\rangle + V_{\rm xc}[\overline{\rho}_{\mu\nu}]\langle\mu|\nu\rangle + V'_{\rm xc}[\overline{\rho}_{\mu\nu}](\langle\mu|\rho|\nu\rangle\\ &- \overline{\rho}_{\mu\nu}\langle\mu|\nu\rangle) - V_{\rm xc}[\overline{\rho_{ij}}]\langle\mu|\nu\rangle - V'_{\rm xc}[\overline{\rho_{ij}}](\langle\mu|(\rho_i + \rho_j)|\nu\rangle\\ &- \rho_{ij}\langle\mu|\nu\rangle)\end{aligned} \tag{24}$$

with

$$\overline{\rho_{ij}} = \frac{\langle w_\mu|(\rho_i + \rho_j)|w_\nu\rangle}{\langle w_\mu|w_\nu\rangle} \tag{25}$$

(indices μ, ν omitted for clarity). In Eqs. (21) and (24) $\overline{\rho}_{\mu\nu}$, which includes all density contributions, is defined using Eq. (19). Equations (19), (21), (22), (24), and (25) form the basis of the McWEDA approximation for the calculation of exchange-correlation matrix elements, and are the important theoretical underpinning of the results we present in the next section. Notice that in this approach the GSN approximation, Eq. (20), is only used to evaluate the corrections [terms inside parentheses in Eqs. (16) and (23)] to the dominant one- or two-center contributions.

IV. RESULTS

In this section we present results illustrating the performance of our exchange-correlation scheme discussed in Sec. III. Figure 1 shows LDA exchange-correlation matrix elements for a Si dimer (along the z axis), as a function of distance, calculated using the different approximations discussed in Secs. II and III. Figure 1(a) shows the on-site exchange-correlation-energy matrix element $\langle p_z|\epsilon_{\rm xc}|p_z\rangle$: the solid line represents the exact result, the dashed line our approximation [Eq. (21)], and the dotted line the original SN average density approximation [see Eq. (45) in Ref. 1]. In

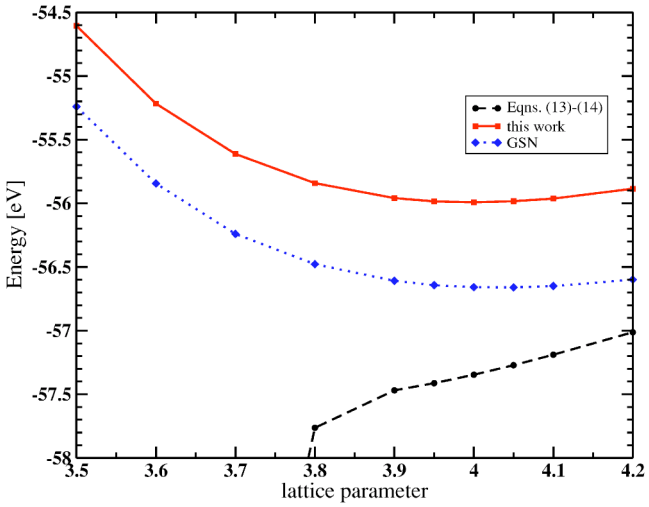

FIG. 2. (Color online) Total energy for bulk Al as a function of the lattice parameter a. LDA exchange-correlation matrix elements are calculated using different approximations. The solid line ("This work") corresponds to McWEDA Eqs. (21) and (24); the dashed line to Eqs. (13) and (14) [i.e., the Horsfield approximation without the correction of Eq. (15)]; and the dotted line is the GSN approximation Eq. (20). These calculations are performed using the FIREBALL code and a basis set of Al sp^3 fireball orbitals with cutoff radii $R_c(s)=5.3$ a.u., $R_c(p)=5.7$ a.u.

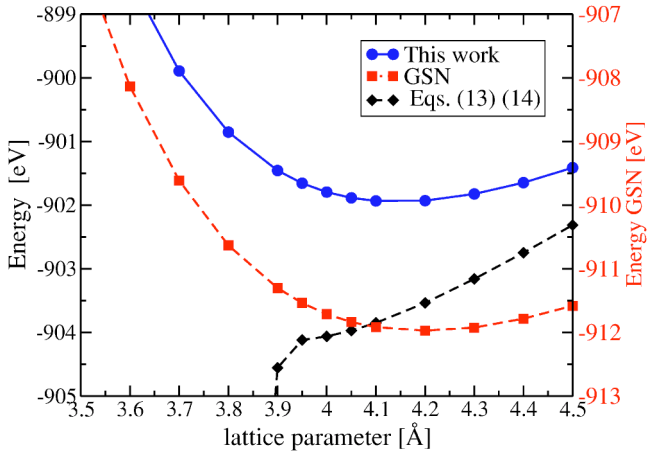

FIG. 3. (Color online) Total energy for bulk Au as a function of the lattice parameter a. LDA exchange-correlation matrix elements are calculated using McWEDA Eqs. (21) and (24) ("This work"); the Horsfield result Eqs. (13) and (14); and Eq. (20) (GSN). The energy scale on the right corresponds to the GSN approximation. These calculations are performed using the FIREBALL code and a basis set of sp^3d^5 fireball orbitals with cutoff radii $R_c(s)=4.6$ a.u., $R_c(p)=5.2$ a.u., and $R_c(d)=4.1$ a.u.

this case, the Horsfield approximation Eq. (13) coincides with the exact result; on the other hand, the SN and GSN methods, Eq. (20), yield identical results. In this figure we observe that the McWEDA approach reproduces with high accuracy ($\sim$1%) the exact result, while the SN approach yields a larger error ($\sim$7%). Notice that the origin of the inaccuracy in using the SN method occurs at large distances and is due to averaging a single atomic density in the atomic limit. The error as a function of distance is practically constant and thus appears as a rigid shift in the total energy curve (e.g., see Figs. 2 and 3). Our McWEDA approach, on the other hand, tends to the exact value in this limit. Similar results are obtained for the other on-site $\langle\mu|\epsilon_{xc}|\mu\rangle$ terms [we present in Fig. 1(a) the case where the largest discrepancies are found].

Figure 1(b) shows the *off-site* matrix elements $\langle p_z(1)|V_{xc}|p_z(2)\rangle$ for the Si dimer. In this case, both the McWEDA Eq. (24) and the Horsfield method Eq. (14) coincide with the exact result (solid line). The original SN approximation [Eqs. (40) and (41) in Ref. 1] is represented by the dotted line: this curve follows closely the exact one, with a deviation of $\sim$3%. Finally, the dash-dotted line shows the GSN result Eq. (20). Although the GSN approximation is only used in the approach presented in this paper to evaluate the correction in Eq. (16), it is instructive to compare it with the original SN approximation. As shown in Fig. 1(b), both approximations yield almost identical results. At very short distances ($(d \leqslant 1.25$ Å, not shown) the SN approximation begins to deviate significantly from both the GSN and exact results. (In fact the SN approximation is not well defined for $d \sim 1.2$ Å where the sign of $\langle\phi_\mu|\rho|\phi_\nu\rangle$ is different from the sign of $\langle\phi_\mu|\phi_\nu\rangle$).

Figure 2 shows the total energy as a function of lattice parameter a for bulk (fcc) Al, as calculated with the FIREBALL code using an sp^3 basis set [fireball orbitals with cutoff

TABLE I. Equilibrium lattice constants a and bulk moduli B for selected elements obtained using McWEDA, Eqs. (21) and (24) ("This work") for the exchange-correlation LDA contributions, using sp^3 (Al,Si) or sp^3d^5 (transition metals) basis sets of fireball orbitals with cutoff radii R_c (in a.u.) as indicated. Also shown are plane-wave LDA and experimental values.

		R_c (a.u.)			a (Å)			B (GPa)		
Name		s orbital	p orbital	d orbital	This work	PW LDA	Expt.	This work	PW LDA	Expt.
Au	fcc	4.6	5.2	4.1	4.14	4.06[a]	4.07	210	170[a]	173
Pd	fcc	4.6	5.0	4.0	3.96	3.94[b]	3.89	215	178[b]	181
W	bcc	4.7	5.2	4.5	3.18	3.14[a]	3.16	347	333[a]	323
Si	dia	4.8	5.4		5.46	5.37[b]	5.43	109	98[b]	99
Al	fcc	5.3	5.7		4.04	3.96[b]	4.05	93	87[b]	72

[a]See Ref. 25.
[b]See Ref. 26.

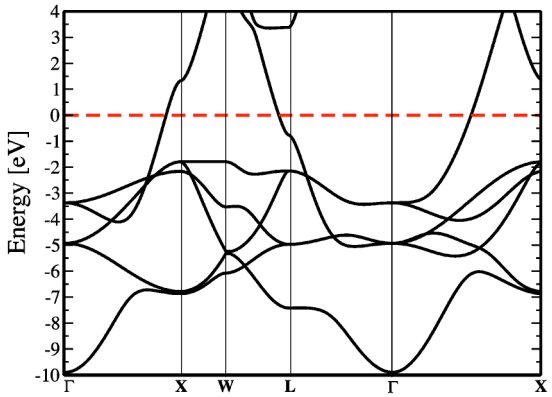

FIG. 4. Band structure of fcc Au. LDA exchange-correlation terms are calculated using the McWEDA approach discussed in Sec. III. Basis set: sp^3d^5 fireball orbitals with cutoff radii $R_c(s)=4.6$ a.u., $R_c(p)=5.2$ a.u., and $R_c(d)=4.1$ a.u. The dashed line represents the Fermi level.

radii $R_c(s)=5.3$ a.u. and $R_c(p)=5.7$ a.u.], using different approximations to calculate the LDA exchange-correlation matrix elements. First of all, notice the critical failure of Eqs. (13) and (14) [i.e., the Horsfield approximation without additional numerical integrals—Eq. (15)]. In this system each atom i has a lot of overlapping neighbors ($j \neq i$), and Eq. (13) does not describe properly the on-site exchange-correlation matrix elements. Our McWEDA approach [Eq. (21)], on the other hand, does not suffer from this problem, as shown by the solid line. This minimal sp^3 basis set calculation yields an equilibrium lattice constant $a=4.04$ Å and bulk modulus $B=93$ GPa, to be compared with the values $a=3.97(4.05)$Å and $B=84(76)$ GPa from plane-wave LDA (PW LDA) calculations (experiment is in parentheses, as shown in Table I). For the sake of completeness, we also show in this figure the total-energy curve corresponding to using the GSN approximation Eq. (20) for the calculation of the exchange-correlation matrix elements [i.e., Eq. (20) instead of Eqs. (21) and (24)]. This curve presents an almost rigid shift ($\sim$0.7 eV) to lower energy values, associated with the calculation of the on-site $\langle\mu|\epsilon_{xc}|\mu\rangle$ terms [see Fig. 1(a)].

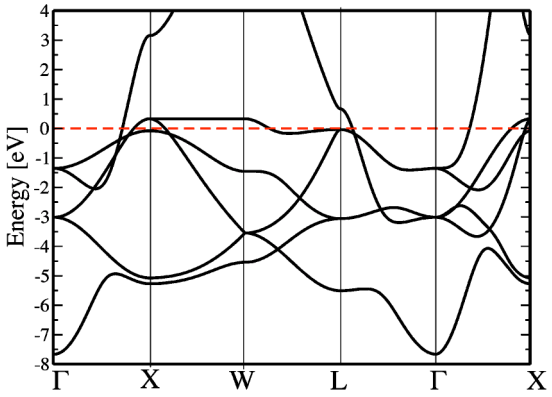

FIG. 5. Band structure of bcc W (see also Fig. 4). Basis set: sp^3d^5 fireball orbitals with cutoff radii $R_c(s)=4.7$ a.u., $R_c(p)=5.2$ a.u., and $R_c(d)=4.5$ a.u.

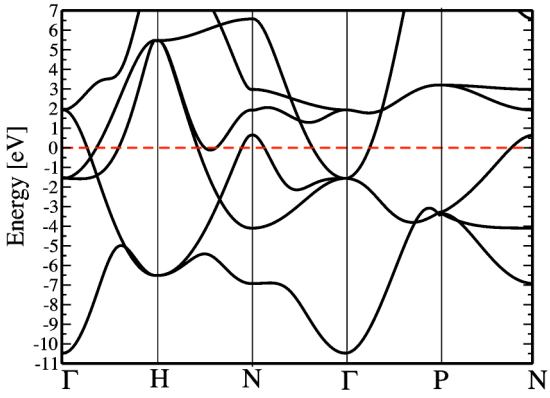

FIG. 6. Band structure of fcc Pd (see also Fig. 4). Basis set: sp^3d^5 fireball orbitals with cutoff radii $R_c(s)=4.6$ a.u., $R_c(p)=5.0$ a.u., and $R_c(d)=4.0$ a.u.

Transition metals contain a significant valence electron density (the d-electrons), mixed with a free-electron-like density (the sp-bands), and thus represent good test cases for the different exchange-correlation schemes. Figure 3 (solid line) shows the total energy of bulk Au as a function of the lattice parameter as calculated with the FIREBALL code using the exchange-correlation scheme proposed in Sec. III [i.e., Eqs. (21) and (24)]. We used an sp^3d^5 basis set with fireball orbitals defined by the following cutoff radii: $R_c(s)=4.6$ a.u., $R_c(p)=5.2$ a.u., and $R_c(d)=4.1$ a.u. In similarity with Fig. 2, we also show the results for GSN [Eq. (20)], and Horsfield [Eqs. (13) and (14)]. These results demonstrate how critical it is for the transition metals to have a good description of the on-site exchange-correlation contributions: the GSN curve (scale on the right of Fig. 3) is now shifted by $\sim$10 eV to lower values,[24] and Eqs. (13) and (14) fail drastically to describe properly the total energy as a function of lattice parameter a. On the other hand, the McWEDA approach yields a fairly good description of bulk Au (see also Table I and Fig. 4).

Table I shows the calculated lattice parameter a and Bulk modulus B_0 (obtained using a Murnaghan equation of state) for Au, as well as for other transition metals (Pd, W), Al (a typical free-electron-like metal), and Si (a typical semiconductor). These results have been obtained using either minimal sp^3 basis sets (Al,Si) or sp^3d^5 basis sets (transition met-

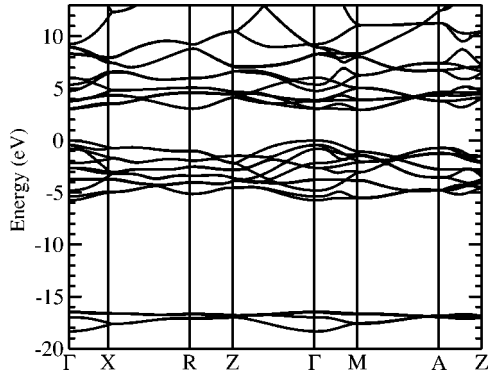

FIG. 7. Band structures for TiO_2 in the rutile structure. The valence-band maximum is taken as the zero of energy.

TABLE II. Comparison of the McWEDA band structures of Figs. 4–6 at selected high-symmetry points with accurate APW LDA (values in brackets) calculations (Ref. 31). All values (in eV) are referred to the Fermi energy.

	Γ_1	$\Gamma_{25'}$	Γ_{12}	N_1	N_2	$N_{1'}$	N_1
W	−10.48 (−10.20)	−1.56 (−1.18)	1.94 (1.90)	−6.92 (−6.53)	−4.10 (−3.54)	0.65 (0.64)	1.92 (1.93)
	Γ_1	$\Gamma_{25'}$	Γ_{12}	L_1	L_3	L_3	$L_{2'}$
Au	−9.90 (−10.29)	−4.93 (−4.62)	−3.37 (−3.14)	−7.42 (−7.40)	−4.95 (−4.72)	−2.17 (−1.92)	−1.17 (−1.09)
Pd	−7.66 (−7.30)	−3.01 (−2.86)	−1.36 (−1.29)	−5.50 (−5.34)	−3.06 (−2.97)	−0.03 (−0.03)	0.67 (0.70)

als). The experimental values[27] and the PW LDA values are also presented in Table I. This table shows that with the McWEDA approach the experimental lattice constants a are reproduced within ~2% while the bulk moduli are slightly overestimated by ~15%. The agreement is improved when comparing with the theoretical PW LDA result. Since the accuracy of first-principles TBMD methods is mainly related to the quality of the atomiclike basis set, improvements of the results presented in Table I are to be expected with a better choice for the basis set, either by improving the sp^3 or sp^3d^5 orbitals and/or by adding new orbitals to the basis set (e.g., double basis sets, etc.).[12,28–30]

Electronic structures from TBMD are often used not only for the calculation of forces and total energies (which require a good description of the electronic structure of the system) but also in studies of optical properties, electronic transport, etc. In order to analyze the accuracy of the McWEDA approach Eqs. (21)–(24) for the calculation of the electronic structure, we show in Figs. 4–6 the electronic band structures for the transition metals Au, W, and Pd, calculated using sp^3d^5 basis sets. As mentioned above, transition metals represent good test cases since they present a mixture of localized (the d electrons) and free-electron-like (the sp bands) states. The comparison with more accurate calculations (e.g., see Ref. 31) shows a very good overall agreement. For a more detailed comparison, Table II shows the values of these electronic structures (Figs. 4–6) at selected high-symmetry points as compared with augmented plane-wave (APW) LDA calculations.[31]

Tetragonal rutile structure TiO_2 belongs to the space group $P4_1/mnm$, containing six atoms per unit cell. The structural parameters for rutile structure TiO_2 have been determined to a high degree of accuracy from the neutron diffraction experiments performed by Burdett *et al.*[32] We have calculated the structural parameters and electronic band structure for TiO_2 in the rutile structure using the FIREBALL code and the exchange-correlation approach discussed in Sec. III. For these calculations we have used an sp^3 basis for oxygen with cutoff radii $R_c(s)=3.6$ a.u. and $R_c(p)=4.1$ a.u., while for Ti a basis set of sp^3d^5 orbitals was used, with cutoff radii $R_c(s)=6.3$ a.u., $R_c(p)=6.0$ a.u., and $R_c(d)=5.7$ a.u. The optimal structure is obtained by minimizing the total energy of the rutile ($P4_1/mnm$) structures with respect to the lattice parameters a,c and the internal parameter u. We perform this minimization by a two-step procedure as outlined in Ref. 33. Table III summarizes the comparison of our results to the experimentally determined structural and elastic parameters in TiO_2, and other theoretical work. This table shows that our results for the structural properties of TiO_2 in the rutile structure are within 1% of the experimental results of Burdett *et al.*[32] From the equation of state, we obtain a value for the bulk modulus B of 206 GPa which agrees well with the experimental value of 211 GPa.[34] In addition, our results agree well with the calculated results of others.[33,35]

Using our theoretically predicted equilibrium lattice parameters, we have calculated the self-consistent electronic band structure for rutile TiO_2 depicted in Fig. 7 along the high-symmetry directions of the irreducible Brillouin zone. Table IV gives a summary of our results in comparison to experiment and other calculations for the detailed features of the band structure. The upper valence band is composed of O $2p$ orbitals and has a width of 5.75 eV. These results are in agreement with the experimental values of 5.50 eV.[36] The lower O $2s$ band is 1.89 eV wide. Our results are consistent with other calculations.[33,35] The calculated direct band gap at Γ of 3.05 eV is in agreement with the reported experimental

TABLE III. Theoretical results for structural and elastic parameters for TiO_2 in the rutile structure. Comparisons are made between our results (McWEDA) and experimental results for the volume V, lattice parameters a,c, internal parameter u, and bulk modulus B; zero subscript represents the experimental results (Ref. 32).

	V/V_0	a/a_0	c/c_0	u/u_0	B (GPa)	B_0 (GPa)[a]
Present work	0.994	0.997	0.999	0.994	206	211
Other calculation[b]	1.039	1.013	1.002	1.001	240	
Other calculation[c]	1.021	0.999	1.002	0.998	209	

[a]See Ref. 34.
[b]See Ref. 33.
[c]See Ref. 35.

TABLE IV. Comparison of our present work to the experimentally determined electronic properties for TiO_2 in the rutile structure. Definition of listed quantities are as follows: (1) E_g (D) is the direct band gap (Γ to Γ), (2) E_g (ID) is the indirect band gap (Γ to M), (3) E_{VB} is the upper valence bandwidth, and (4) $E_{O\ 2s}$ is the oxygen 2*s* state bandwidth.

Structure	E_g (D) (eV)	E_g (ID) (eV)	E_{VB} (eV)	$E_{O\ 2s}$ (eV)
Present	3.05	2.92	5.75	1.89
Experiments	3.06[a]		5.50[b]	
Others	1.78,[c] 2.00[d]	3.00,[c] 2.00[d]	6.22,[c] 5.7[d]	1.94,[c] 1.80[d]

[a]See Ref. 37.
[b]See Ref. 36.
[c]See Ref. 35.
[d]See Ref. 33.

gap of 3.06 eV.[37] This agreement is the result of multiple errors (the local density approximation, the Kohn-Sham approximation,[38] our approximation of the exchange-correlation matrix elements, and the local orbital basis set) that tend to oppose one another. The traditional use of the LDA and the Kohn-Sham approximation generally underestimates (compared to experiment) the band gap for insulators and semiconductors.[39,40] The band gap obtained from PW LDA calculations for TiO_2 is $\sim$2.0 eV.[33] Finite local orbital basis sets tend to overestimate band gaps; that, in addition to our approximations, along with the LDA and Kohn-Sham errors produces the present band gap of 3.05 eV.

We also find an indirect band gap from Γ to M which is smaller than the direct band gap by 0.13 eV.

V. SUMMARY

In summary, we have presented an improved approach to calculate exchange-correlation contributions in first-principles TBMD methods. After a brief presentation of the basic theoretical foundations and practical motivation for these techniques, we have discussed the different approximations [SN (Ref. 1) and Horsfield[5]] used so far to calculate exchange-correlation terms in these methods, using standard DFT (e.g., LDA). Then, in Sec. III, we propose an alternative approach that corrects the main deficiencies of previous approximations in a practical manner, keeping always in mind computational efficiency. In this approach, on-site (off-site) exchange-correlation matrix elements are formally written as a one-center (two-center) term plus a correction due to the rest of the atoms. The one-center (two-center) term is evaluated (and tabulated) directly, while the correction is calculated using a SN-like approach. For this purpose, a general (i.e., for arbitrary atomiclike basis set) version of the SN approach has also been developed. We refer to our methodology as the multicenter weighted exchange-correlation density approximation.

The scheme has been tested for several materials using the FIREBALL code and minimal sp^3 (for Al, Si, and O) or sp^3d^5 (Au, Pd, W, and Ti) basis sets. The results, presented in Sec. IV, show the good accuracy of the present first-principles TBMD approach as compared with experiment and other accurate calculations.

ACKNOWLEDGMENTS

P.J. gratefully acknowledges financial support by the Spanish Ministerio de Educacion, Cultura y Deportes. This work has been supported by the DGI-MCyT (Spain) under Contracts No. MAT2001-0665 and No. MAT2004-01271. J.P.L. and H.W. gratefully acknowledge financial support from DOE Grant No. DE-FG02-03ER46059 and from the Center for the Simulation of Accidental Fires and Explosions (C-SAFE at the University of Utah), funded by the Department of Energy, Lawrence Livermore National Laboratory, under Subcontract No. B341493. O.F.S. thanks the NSF (Grant No. DMR 99-86706) for support.

[1] O. F. Sankey and D. J. Niklewski, Phys. Rev. B **40**, 3979 (1989).
[2] P. Hohenberg and W. Kohn, Phys. Rev. **136**, B864 (1964).
[3] W. Kohn and L. J. Sham, Phys. Rev. **140**, A1133 (1965).
[4] J. P. Perdew, in *Electronic Structure of Solids '91*, edited by P. Ziesche and H. Eschring (Akademie Verlag, Berlin, 1991), p. 11.
[5] A. P. Horsfield, Phys. Rev. B **56**, 6594 (1997).
[6] A. P. Horsfield and A. M. Bratkovsky, J. Phys.: Condens. Matter **12**, R1 (2000).
[7] D. Porezag, Th. Frauenheim, Th. Kohler, G. Seifert, and R. Kaschner, Phys. Rev. B **51**, 12 947 (1995); T. Frauenheim, F. Weich, Th. Kohler, S. Uhlmann, D. Porezag, and G. Seifert, *ibid.* **52**, 11 492 (1995).
[8] P. Ordejon, E. Artacho, and J. M. Soler, Phys. Rev. B **53**, R10 441 (1996); D. Sanchez-Portal, P. Ordejon, E. Artacho, and J. M. Soler, Int. J. Quantum Chem. **65**, 453 (1997).
[9] P. Pou, R. Oszwaldowski, H. Vázquez, R. Pérez, F. Flores, and J. Ortega, Int. J. Quantum Chem. **91**, 151 (2003); R. Oszwaldowski, H. Vázquez, P. Pou, J. Ortega, R. Pérez, and F. Flores, J. Phys.: Condens. Matter **15**, S2665 (2003).
[10] J. Ortega, Comput. Mater. Sci. **12**, 192 (1998).
[11] H. Eschrig and I. Bergert, Phys. Status Solidi B **90**, 621 (1978).
[12] J. Junquera, O. Paz, D. Sánchez-Portal, and E. Artacho, Phys.

Rev. B **64**, 235111 (2001).
[13] J. Ortega, R. Pérez, and F. Flores, J. Phys.: Condens. Matter **12**, L21 (2000).
[14] J. Ortega, F. Flores, and A. L. Yeyati, Phys. Rev. B **58**, 4584 (1998).
[15] A. A. Demkov, J. Ortega, O. F. Sankey, and M. P. Grumbach, Phys. Rev. B **52**, 1618 (1995).
[16] J. P. Lewis, K. R. Glaesemann, G. A. Voth, J. Fritsch, A. A. Demkov, J. Ortega, and O. F. Sankey, Phys. Rev. B **64**, 195103 (2001).
[17] J. Harris, Phys. Rev. B **31**, 1770 (1985).
[18] W. M. Foulkes and R. Haydock, Phys. Rev. B **39**, 12 520 (1989).
[19] J. P. Lewis, J. Pikus, Th. E. Cheatham, E. B. Starikov, H. Wang, J. Tomfohr, and O. F. Sankey, Phys. Status Solidi B **233**, 90 (2002).
[20] F. J. García-Vidal, J. Merino, R. Pérez, R. Rincón, J. Ortega, and F. Flores, Phys. Rev. B **50**, 10 537 (1994).
[21] P. Pou, R. Pérez, F. Flores, A. Levy Yeyati, A. Martin-Rodero, J. M. Blanco, F. J. García-Vidal, and J. Ortega, Phys. Rev. B **62**, 4309 (2000).
[22] Typically, the time spent in the generation of data tables is five times longer in the Horsfield approach, as compared with the SN method.
[23] Note that since the functions w_{il} are spherically symmetric, the same value of $\overline{\rho}_{\mu\nu}$ is obtained for all the orbitals (μ,ν) associated with a given pair of atomic subshells $(i,l;i',l')$; this result is consistent with the spherical approximation used in the calculation of the Hartree terms.
[24] As mentioned above, this shift is related to the inaccuracy of the average-density approximation for calculating the on-site energy terms $\langle\mu|\epsilon_{\mathrm{xc}}|\mu\rangle$: Au atoms contain a large electron density (~ten d electrons plus one s electron) in the valence band. For comparison, this shift is only ~0.7 eV in the case of bulk Al (see Fig. 2).
[25] L. Shi and D. A. Papaconstantopoulos, Phys. Rev. B **70**, 205101 (2004).
[26] A. García, Ch. Elsasser, J. Zhu, S. G. Louie, and M. L. Cohen, Phys. Rev. B **46**, 9829 (1992).
[27] C. Kittel, *Introduction to Solid State Physics*, 6th ed. (Wiley, New York, 1986).
[28] S. D. Kenny, A. P. Horsfield, and Hideaki Fujitani, Phys. Rev. B **62**, 4899 (2000).
[29] E. Anglada, J. M. Soler, J. Junquera, and E. Artacho, Phys. Rev. B **66**, 205101 (2002).
[30] T. Ozaki and H. Kino, Phys. Rev. B **69**, 195113 (2004).
[31] D. A. Papaconstantopoulos, *Handbook of the Band Structure of Elemental Solids* (Plenum Press, New York, 1986).
[32] J. K. Burdett, T. Hughbanks, G. J. Miller, J. W. Richardson, and J. V. Smith, J. Am. Chem. Soc. **109**, 3639 (1987).
[33] K. M. Glassford and J. R. Chelikowsky, Phys. Rev. B **46**, 1284 (1992).
[34] T. Arlt, M. Bermejo, M. A. Blanco, L. Gerward, J. Z. Jiang, J. S. Olsen, and J. M. Recio, Phys. Rev. B **61**, 14 414 (2000).
[35] S. D. Mo and W. Y. Ching, Phys. Rev. B **51**, 13 023 (1995).
[36] S. P. Kowalczyk, F. R. McFeely, L. Ley, V. T. Gritsyna, and D. A. Shirley, Solid State Commun. **23**, 161 (1977).
[37] J. Pascual, J. Camassel, and H. Mathieu, Phys. Rev. B **18**, 5606 (1978).
[38] R. M. Dreizler and E. K. U. Gross, *Density Functional Theory* (Springer-Verlag, Berlin, 1990).
[39] K. Vos, J. Phys. C **10**, 3917 (1977).
[40] R. V. Kasowski and R. H. Tait, Phys. Rev. B **20**, 5168 (1979).